Fracture Failure Modes in Lightweight Bearings

John C. Clark*
General Electric Company, Cincinnati, Ohio

Rolling contact bearings fail in a wide variety of different modes. A fracture mode of failure becomes a possibility when operating with significant tensile hoop stress in the races. A series of sixteen bearings operated with tensile stresses in the races were analyzed for cracks. Ten of the sixteen bearings generated cracks of critical size resulting in rapid fracture of the races. From these data, an estimate is made of the critical stress intensity factor for AISI 52100 and AISI M-50, the materials currently used in aircraft engine bearings. Flaws are generated in the races apparently due to a combination of tensile hoop stress and the superimposed Hertz stress pattern. An attempt was made to correlate the flaw size and shape to the known stress fields, or components of the stress fields, but currently these have not been completely successful. Using relatively simple, established fracture mechanic techniques, a limiting stress level can be determined for a given flaw size, but experimental data must be relied upon to predict the flaw size, particularly the depth of the flaw. By proper design, the stresses can be maintained at sufficiently low levels to preclude rapid fracture in the outer races. The area of concern arises in engines of the future with increased rotor speeds which will generate high hoop stresses in the bearing inner races. Bearing materials with increased fracture toughness may be required for these applications.

Nomenclature

σ = stress, PSI
UTS = ultimate tensile strength, PSI
YS = yield strength, PSI
$\bar{r}$ = average ring radius,inches
ω = shaft rotational velocity, rad/sec
$\hat{K}^*$ = cyclic range of stress intensity factor, KSI (in.)$^{1/2}$
$\check{K}$ = threshold value for stress intensity factor, KSI (in.)$^{1/2}$
K_I = plane strain stress intensity factor, KSI (in.)$^{1/2}$
K_{IC} = critical plane strain stress intensity factor, KSI (in.)$^{1/2}$
a = crack depth, in.
c = ½ crack length, in.
Φ = complete elliptic integral of the second kind
x,y,z = subscripts denoting principal stress directions in Hertzian stress field
ρ = mass density, lb-sec^2/in.^{4}
K = proportionality constant
θ = flaw reference angle, deg

Introduction

THE requirements for aircraft engines with increased thrust-to-weight ratios, demands lightweight bearings and supporting structures of ever increasing thinness which become very flexible. In the extreme case the bearings become almost integral with the support structure. This reduction in structural stiffness introduces bending stress into the outer races of the bearings. Future engines, of the 1980's, probably will have an added requirement for bearing *DN*'s approaching 3.0 million (*DN* is a bearing speed parameter similar to tip speed, and is equal to the product of the bearing bore in millimeters and the shaft speed in rpm). Such high shaft speeds introduce significant hoop tensile stresses into the bearing inner races. Both situations can lead to much more rapid crack growth than normal and result in complete fracture of the races in very short order. Such failures normally result in extensive secondary damage to the engine.

Bearings fail in a wide variety of different modes, surface fatigue, subsurface fatigue, plastic flow, etc. These have been investigated and are well tabulated.[1] The classical failure mode, however, is subsurface fatigue. In this failure mode a small crack forms subsurface, normally associated with a stress riser such as a void, nonmetallic inclusion, or carbide. The crack propagates radially outward from this point of initiation and upon reaching the surface forms a spall. Quite often this crack will simultaneously propagate radially inward from the same point of origin, but such growth does not reach significant depths. It is assumed that the cracks which initiate rapid race fractures are of the exact same nature, but do not arrest. Instead the superimposed hoop tensile stress field permits them to propagate to the surface and throughout the Hertzian stress field. Rapid fracture results from high levels of stress above what we will henceforth term "safe operating" stress levels.

This paper presents a simplified approach for estimating safe operating stress levels. Rather than approaching the problem from a theoretical view, we draw heavily upon a number of experimental bearing test results from test rigs or engines, where race cracks were generated, and from these develop an empirical estimation technique. In some cases, tests were terminated before the cracks became critical in size and thus before rapid fracture occurred. In others, generally where outer race cracks were experienced, the races quickly fractured leading to loss of rotor axial restraint. Table 1 is a tabulation of the failure experience used. This table will be frequently referenced throughout this paper.

Figure 1a is a schematic representation of crack growth rate as a function of stress intensity range. Since these type data have not been specifically developed for bearing materials, the diagram is used only to introduce the rapid fracture problem. When the bearings are operated at low hoop stress levels, the stress intensity range is below the propagation threshold value ($\hat{K}^*$). Thus the cracks formed do not propagate or the propagation rate is sufficiently slow that normal spalling fatigue will develop. While spalling is undesirable, it is a relatively gradual failure process that can be detected by vibration monitors, chip detection, or other oil system monitors and consequently the affected components can usually be removed before more serious secondary damage is incurred. However, as the stress level, and thus the stress intensity range, increase, the crack growth rate accelerates until a

Received October 15, 1974. The early investigation of race cracking and the application of fracture mechanics to determine possible safe stress levels was conducted by R. E. Johnson of the Aircraft Engine Group of General Electric. A great deal of additional work involving the application of fracture mechanics to bearings has been accomplished by Johnson and others, but is not reported here because of the general nature of the assumptions used to estimate rapid fracture thresholds.

Index categories: Materials, Properties of; Structural Stability Analysis; Structural Static Analysis.

*Manager, Bearing and Seal Design and Material Technology.

Table 1 Tabulation of the failure experience

Bearing number	Material	Stress level (ksi)	Crack depth (in.)	Crack length (in.)	Stress intensity factor K_I	Type bearing	Description	Result
1	AISI M50	37	0.11	0.40	19.2	thrust	O. Race 7 cases—slight spalling (4) —no spalling (3)	fracture fracture
2	AISI M50	30	0.140	0.33	15.0	thrust	O. Race heavy spalling—outer race restrained by housing	fracture
3	AISI 52100	26.5	0.174	0.532	16.7	roller	I. Race no spalling	fracture
4	AISI M50	22.5	0.057	0.21	8.4	roller	I. Race slight spalling	fracture
5	AISI M50	15	0.090	0.320	7.0	thrust	O. Race 2 cases—slight spalling	no fracture
6	AISI 52100	26.5	0.14	0.350	13.87	roller	I. Race no spalling	no fracture
7	AISI M50	27.0	0.110	0.320	13.0	thrust	I. Race 3-in. spall	no fracture
8	AISI M50	27.0	0.120	0.330	13.4	thrust	I. Race 2-in. spall	no fracture
9	AISI M50	24.5	0.170	0.505	14.5	thrust	I. Race no spalling	no fracture

point is reached where the stress intensity factor is large enough to produce rapid fracture and is said to reach its critical value. Figure 1b is another schematic representation showing the effects of hoop stress. The time scale represents operating time measured from the initiation of a subsurface defect. At low stress levels, spalls form and if not detected by the aforementioned methods, the vibration or impact damage will eventually lead to cage failure. This is normally the final stage of a bearing failure. At increased stress levels, rapid fracture occurs prior to significant spalling and consequently no warning is given. It is very likely that time to spall is decreased by increasing the stress level; but for the purpose of this diagram it is assumed independent of hoop stress.

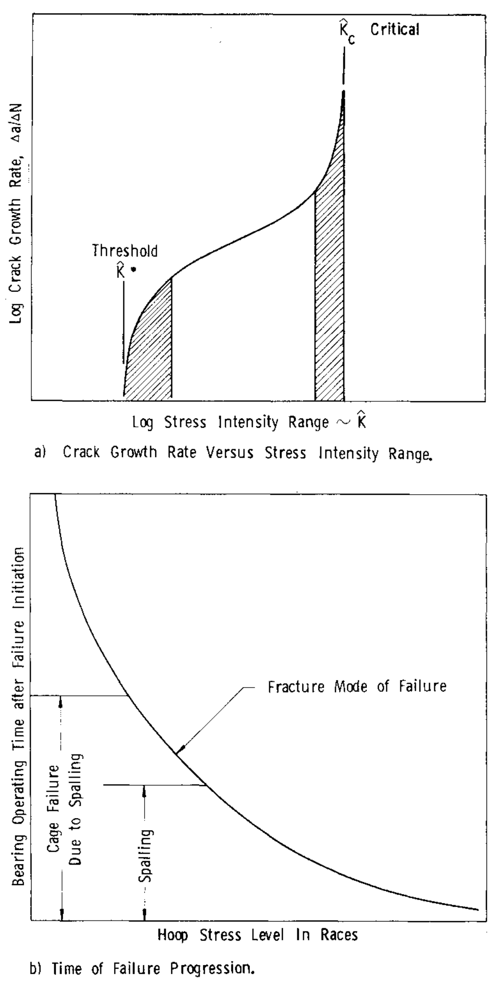

Fig. 1 Schematic representation of crack growth rate vs stress intensity range and representation of time of failure propagation.

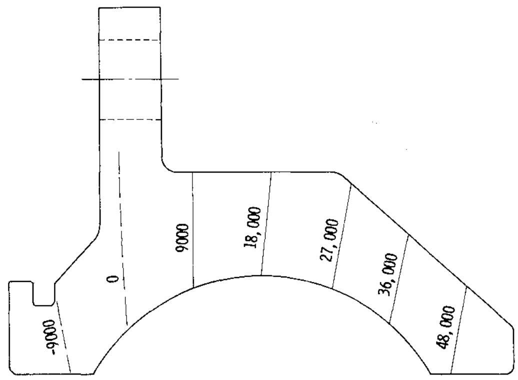

Fig. 2 Bearing no. 1 outer race cross section and stress distribution. Ball diameter = 1.625 in. Bearing pitch diameter = 10.827 in.

Outer Race Stress Levels

Before discussing the aspects of rapid fracture, it would be beneficial to understand the stress state of both inner and outer races. If the outer race is directly mounted to the bearing housing or frame (bolted flange bearing), this race essentially becomes an integral part of the structure and, as such, will reflect bending load and stress levels similar to those in the structure. Figure 2 shows a sketch of the outer race of a bearing bolted directly to the frame in this manner. This race has been analyzed by means of a finite-element computer program for loads resulting from the unbalanced rotor thrust load. In this analysis the load was introduced as a linear axisymmetric load concentrated at the center of the contact zone and operating in the direction of the outer race contact angle. Isostress stress lines are shown for the load levels used in the rig for the fatigue testing. The stress predicted agreed with the measured stress within 5% in the circumferential (hoop) direction. This is the stress of primary interest. An additional alternating stress component of ±5% due to ball passing loads was measured, which could not be determined from the computer analysis. The bearing race shown in Fig. 3 is from a more conventional bearing, but it is a lightweight configuration, mounted to a lightweight housing. The same computer analysis was conducted on this race and the results are shown in Fig. 3.

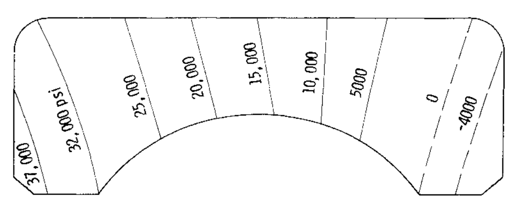

Fig. 3 Bearing no. 2 outer race cross section and stress distribution. Ball diameter = 0.875 in.

Inner Race Stresses

Inner race stresses are primarily a function of the amount of interference resulting from the press fit of the race to shaft, and from the centrifugal loading due to shaft rotation. Inner race fracture is a well-known mode of failure in many industrial applications where tapered inner bores and shafts are used, and the inner race to shaft interference is determined by the amount of torque applied to a drive nut. In aircraft application, fit ups are carefully selected and thus inner race stresses only become a problem when very high speeds are encountered as the "fit" stresses can be limited to small values.

Centrifugal stresses in bearing inner races can be approximated by some simple relationships to identify the threshold stress range for rapid fracture failure modes. Aircraft engine bearing inner races tend to be rings with inner to outer diameter ratios of 1.07 to 1.10. Therefore, it is fairly accurate to treat them as thin rings and to calculate an average tangential stress due to rotation. The stress in a rotating free ring is given by

$$\sigma = \rho r^2 \omega^2 \tag{1}$$

Adjusting for the fact that DN is expressed in terms of the inner diameter of the ring, the equation can be rewritten

$$\sigma = K\rho(DN \times 10^{-6})^2 \tag{2}$$

For bearings typically used in jet engines for a wide variety of shapes and materials the equation becomes

$$\sigma = 3700\ (DN)^2 \tag{3}$$

where DN is given in millions.

Experience has shown that rotating inner rings must maintain a tight fit at operational stress levels if proper life is to be expected. Operating with excessive looseness may allow the inner race halves to become eccentric with resulting high vibration and failure due to ball contact with the inner race split line. Heavy fretting also occurs with loose fit-up, and race to shaft rotation causes severe damage with loose fit-up. This required tight fit-up adds an additional hoop prestress that is superimposed on the centrifugal hoop stress. The amount of press fit varies with bearing size, and the prestress is obviously a function of this fit, bearing size, the shaft configuration and the mechanical properties. No simple, straightforward method exists for determining this stress. To illustrate how this stress might be estimated, however, a typical 150 mm bearing with an operating fit of 0.0015″ at all speed conditions was analyzed and found to have a press fit stress of approximately 5300 psi. Adding this value to Eq. (3) yielded the results shown in Fig. 4. The stresses calculated and tabulated in Table I for inner races resulted from a more accurate analysis which considered the actual bearing size, fit and speed. Generally, small bearings will see higher prestress from press fits. The curve in Fig. 4 is included to show the problems that will arise as shaft speeds increase.

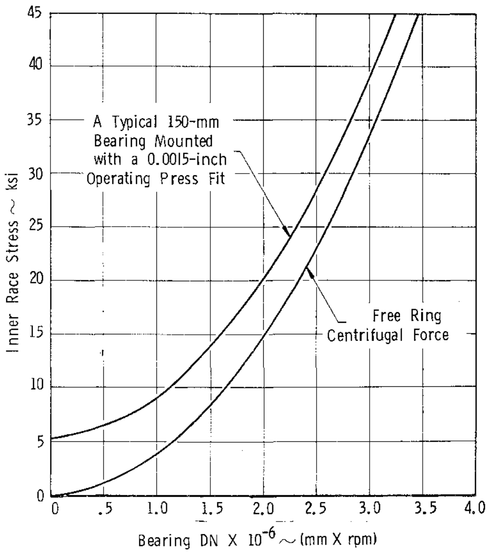

Fig. 4 Estimated inner race tangential stress vs bearing DN.

Simplified Fracture Mechanics Analysis

The analytical method used to predict rapid race fracture and to determine if a safe stress limit could be defined, incorporated the following equation[2] for the plane strain stress intensity factor:

$$K_I = \frac{1.1\sigma(\pi a)^{1/2}}{(\Phi^2 - 0.212(\sigma/\sigma_{ys})^2)^{1/2}} \tag{4}$$

where

$$\Phi = \int_0^{\pi/2} \left(1 - \frac{c^2 - a^2}{c^2} \sin^2 \theta\, d\,\theta\right)^{1/2}$$

The second term in the denominator of Eq. (4) is a correction factor for plastic zone size. Because of the close proximity and high values of the UTS and YS of the two most commonly used aircraft engine bearing materials, AISI M50 and AISI 52100, and the relatively low operating stress levels, this correction factor has little effect on the value of K_I. Equation (4) was developed for semielliptical surface cracks, and was applied in this investigation within the following limits: crack depth (a) $\leq$ 1/2 race thickness; crack depth (a) $\leq$ (C) = 1/2 crack length; and area of crack $\leq$ 10% area of race.

The first term in the denominator Φ being a complete elliptic integral of the second kind, takes on values from 1.0 to 1.5708. The minimum value occurring when $a = c$ (the crack is a semicircle). The denominator of Eq. (4) can be written as

$$Q = \Phi^2 - 0.212\ (\sigma/\sigma_{ys})^2 \tag{5}$$

where Q becomes a flaw shape parameter containing crack geometry and plastic zone correction factor. Then using Eq. (4), the following expression can be written

$$K_I^2 = 1.21\ \pi\sigma^2\ (a/Q) \tag{6}$$

From the group of failures (tabulated in Table 1), dimensions of the cracks were determined and utilizing calculated stress levels the plane strain (K_I) stress intensity factors were calculated using Eq. (4). Also the values of Q (flaw shape parameter) were determined. For analyzing a group of data such as Table 1, it is beneficial to plot the above equation on a log-log plot (Fig. 5). By examining the data on Fig. 5 it appears that the stress intensity factor becomes critical ($K_I = K_{Ic}$) at a value of K_I of approximately 16 KSI (in.)$^{1/2}$. It should be noted that Eq. (4) was developed for a uniform stress field which is applicable only for inner races. For outer races, stress gradients exist as shown by Figs. 2 and 3. As expected, the cracks appear to grow in the direction of the increasing stress gradient. For example, Fig. 6 shows a crack which led to complete fracture of an outer race with the stress pattern shown in Fig. 3. For the outer race cracks, the value of K_I is approximated by using the maximum stress along the crack front. Figure 7 is a photograph of an inner race crack without fracture in a uniform stress field of 27,000 PSI.

One very important question remains unanswered from the data gathered to date. Are the cracks found before

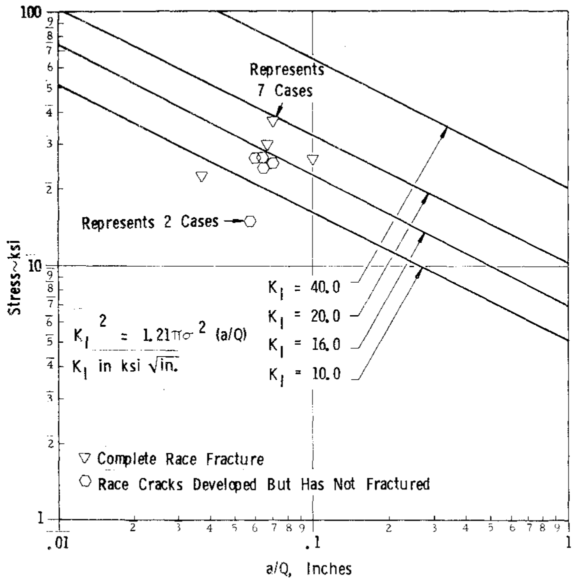

Fig. 5 Graphical solution for stress intensity factors.

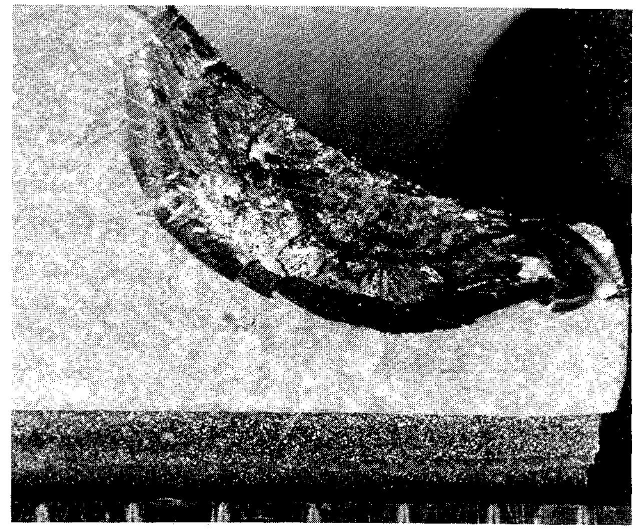

Fig. 7 Inner race crack of bearing operated at 27,000 psi tangential stress giving a K_I − 13.4 ksi (in.)$^{1/2}$ bearing No. 8, Table 1.

growth arrested, or was the bearing removed from service prior to the crack reaching a critical size? To answer this question, the exact mode of crack propagation must be understood. The shape and the appearance of the cracks suggest that the rolling element Hertzian stress field when superimposed over the hoop tensile stress provides the principal crack propagation stress. The surface length of the cracks are usually proportional to the width of the rolling element contact zone, although some reached critical depths before reaching this length. The crack depth, however, has not been uniquely related to any characteristic of the Hertzian stress field.

Crack Initiation

In our early investigations of fractured races, we considered that the cracks initiated from fatigue spalls. However, later evidence indicated that the cracks were very likely the initiation sites for spalling. As can be seen from Table 1, a significant number of incidents have been observed where cracks were present without spalling evidence. In all cases where spalling is present, the crack appears near the leading edge of the spalled area indicating the crack appeared first and initiated the spalling of the raceway.

In the subsurface fatigue spalling mode, two different shear stresses have historically been cited as the cause for the initiation of fatigue fractures. The orthogonal shear stress which occurs on a plane parallel to the surface, has an absolute value equal to about 25% of the maximum surface compressive stress, and is fully reversed as a rolling element passes. This was the original theory on which bearing life was predicted, and many investigators still adhere to this premise. The maximum unidirectional shear stress occurs at a depth slightly greater than the orthogonal shear stress and has a value of about 32% of the maximum surface compressive stress. The maximum unidirectional shear stress can be expressed as $1/2(\sigma_y - \sigma_z)$. Since the hoop stress is in the same plane as σ_y, the hoop stress increases the value of the shear stress by 1/2 of the applied hoop stress. The Hertzian and shear stress analysis follows the development given in Ref. 3. Without going into the details, which are given in Ref. 4, the orthogonal shear stress is not affected by a uniform hoop stress, and thus the unidirectional maximum shear stress appears to be the only influence on crack initiation.

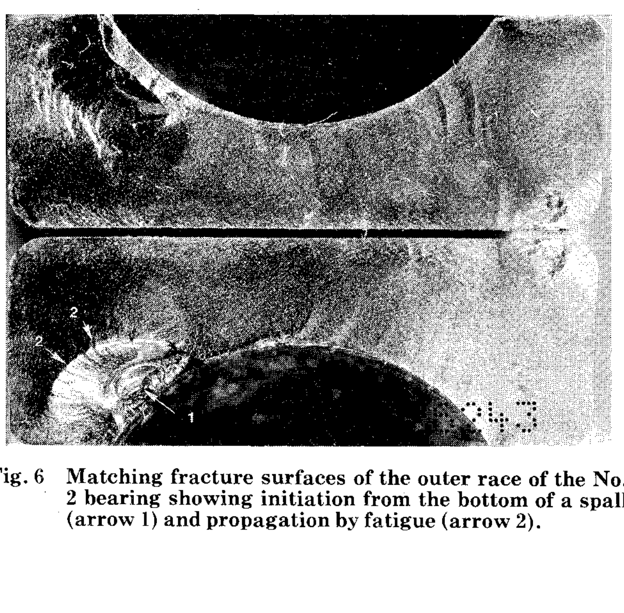

Fig. 6 Matching fracture surfaces of the outer race of the No. 2 bearing showing initiation from the bottom of a spall (arrow 1) and propagation by fatigue (arrow 2).

Crack Propagation

As stated above the Hertzian stress field superimposed over a tensile stress field is assumed to provide the impetus for crack propagation. First, consider a uniform stress field with some microscopic flaw below the surface. A rolling element passing over this flaw introduces a three-dimensional stress array with the three principal stresses in compression. In bearings of normal geometry, one of the principal stresses (σ_y) falls in the plane of the tensile stress field. Therefore in the zone beneath the contact area, the stress patterns in the σ_y plane (hoop) will be

$$\sigma = \sigma_h + \sigma_y \quad \text{when under rolling element load}$$

$$\sigma = \sigma_h \quad \text{between rolling elements}$$

Since σ_y will be highly compressive, we have an alternating stress at element passing frequency from very high compression, to a tensile value equal to the applied hoop stress. For current engines this frequency will accumulate between 10^6 and 10^7 per hour of operation.

Second, the Hertzian stress pattern decays with depth into the race. It would be expected that if the crack propagated out of the Hertzian stress field, the stress intensity factor would drop below the threshold value and the crack would "arrest." To this point it has been assumed that the crack does not significantly alter the Hertzian stress distribution. While this assumption is not completely true, it will not likely cause a large variation until spalling occurs at the surface. At that time the Hertzian pattern will become highly distorted, and stresses due to impact of the rolling element may become significant.

Assuming this hypothesis describes the actual mode of crack propagation, the crack would continue to propagate until σ_y becomes significantly less than σ_h. Several cracks listed in Table 1 have propagated to greater depths than predicted for the value of σ_y however. If there is significant spalling, the crack may be arrested due to the distortion of the Hertzian zone, but this cannot be predicted analytically. Additional work may permit a correlation of the maximum crack depth as a function of the Hertzian and hoop stress patterns.

A unique test was run with applied tensile and compressive stresses to determine what effect each of these stresses has on bearing fatigue life.[5] Each of the tensile stress specimen failed in a rapid fracture mode. These tests were run using a biaxial stress field, but the fractures were normal to the tangential stress (145 KSI) and parallel to the axial stress (128 KSI). It was reported,[5] that it was not clear if a spall developed first or if the fracture occurred prior to spalling. While these stress levels are far in excess of what will occur under normal conditions of load and speed, it is interesting to note that by extending the curve in Fig. 5 to this stress level and assuming a K_{Ic} of 16 KSI $(\text{in.})^{1/2}$, a crack of 5 to 8 mils would be critical in size. In this test, the maximum unidirectional shear occurred at a depth of 5 mils, or the first crack to reach the surface would likely be of critical size and result in rapid fracture.

Discussion

Because of the relative ruggedness of bearings used in the current engine designs, rapid fracture failure modes have not been wide spread. The rotor speeds of today's engines are in the range of 2.0 million *DN* or less and, by examining the curve in Fig. 4, operation has been very successful at tensile stress levels up to approximately 20,000 psi. However, it should be noted that increasing shaft speeds 2.0 to 3.0 million *DN* approximately doubles the inner race operating stress levels. At 3.0 million *DN*, rapid fractures would be expected prior to significant spalling and failure warning time may be extremely short. It is not possible to give a precise stress limit to preclude rapid fracture under these circumstances since the initial flaw size must be known beforehand.

The races tested in tension as reported by Kepple and Mattson[5] appear to have substantially lower fatigue life if the rapid fracture is actually the result of the same subsurface crack that would cause spalling. The data used in the current paper, however, are not sufficiently conclusive to state that this is a definite trend. However, in most cases: 1) the fracture or crack will appear earlier than normal fatigue spalling would be anticipated; 2) the fatigue spalling appears to occur much earlier if tensile stresses result in a stress intensity factor above the threshold value; and 3) the time between crack initiation and propagation to the surface is certainly decreased by the higher stress level.

As stated earlier, through proper designs, outer race stresses can be controlled to prevent rapid fracture. However, as rotor speeds increase, the centrifugal stress acting on the inner race will very likely become a problem that may require new materials, or at least a different approach to the processing of currently used bearing materials.

A brief description of the bearings which have shown cracks and fractures is given in Appendix I.

Conclusions

1) High tensile stress in bearing races will result in rapid fracture, and established fracture mechanics techniques may be used for analysis.

2) The lightweight bearing and support structure must be carefully analyzed to prevent rapid fracture of the outer race.

3) The use of current bearing materials for significantly increased rotor speeds may result in rapid fracture of inner races.

4) The development of bearing materials with improved fracture toughness appears to be a requirement for lightweight bearings with very high rotational speeds. Currently available bearing materials have critical plane strain stress intensity factors of approximately 16 KSI $(\text{in.})^{1/2}$.

5) While the data presented here may be useful as a design guide, estimates of stress intensity factors and operating stress levels should be confirmed with actual data and test for a particular bearing application.

Appendix I: Description of Bearings Listed in Table 1

The bearings listed in Table 1 are a compilation of results both from engine and rig testing. Bearing number one actually represents a sample of 7 bearings run at overload conditions for fatigue (rolling contact) life. These were discussed in a previous paper by C. C. Moore[6] of the General Electric Company. Photographs in Ref. 6 show the nature of the fracture. The stress patterns shown in Fig. 2 represent the test rig conditions. Bearing No. 2 ran in an engine, and is mounted in a low alloy steel housing. The race was restrained by the housing and the fracture was not catastrophic with only a single axial fracture as shown in Fig. 7. The bearing failed by excessive spalling and was detected and removed from the engine. Bearing No. 4 failed at a low stress intensity ratio based on the steady-state stresses calculated and shown in the Table. In this particular bearing the primary source of stress in the inner race is thermal incompatibility, and it is theorized that the stresses may have been much higher transiently. Bearings 5 through 9 represent parts in which well defined cracks were formed, but did not become critical in size.

References

[1]Tallian, T. E., "On Competing Failure Modes in Rolling Contact," *ASLE Transactions*, Vol. 10, Oct. 1967, pp. 418–439.

[2]Irwin, G. R., "The Crack Extension Force for a Part Through Crack in a Plate," *ASME Transactions, Journal of Applied Mechanics*, Series E, Vol. 29, Dec. 1962, pp. 651–654.

[3]Jones, A. B., *Analysis of Stresses and Deflections—New Departure Engineering Data*, New Departure Division of General Motors Corp., Bristol, Conn., 1946.

[4]Lundberg, G. and Palmgren, A., "Dynamic Capacity of Rolling Bearings," *ACTA Polytechnica, Mechanical Engineering Series*, Vol. 1, No. 3, 7 1947.

[5]Kepple, R. R., and Matson, R. L., "Rolling Element Fatigue and Macro-Residual Stress," *ASME Transactions, Journal of Lubrication Technology*, Series F, Vol. 92, April 1970, pp. 76–82.

[6]Moore, C. C., Perkins, P. A., and Smeaton, D. A., "Flange Mounted Ball Bearing Fatigue Test," *ASME Transactions, Journal Basic Engineering*, Series D, Dec. 1967, pp. 919–931.